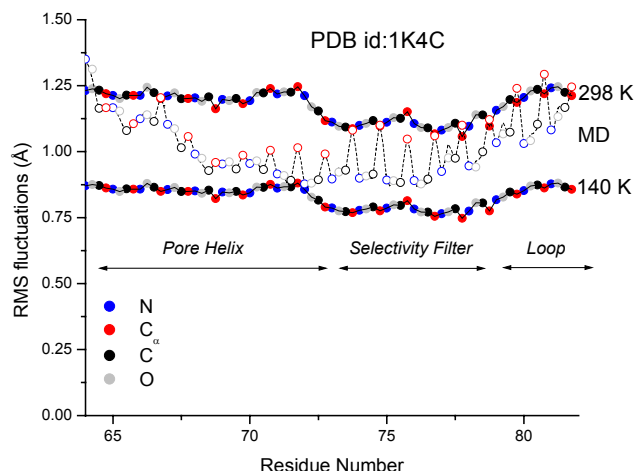


# Supplementary material.

## A) Crystallographic thermal B-factors of the KcsA channel



The RMS atomic fluctuations (defined as  $\langle \Delta R^2 \rangle^{1/2}$ ) extracted from the isotropic Debye-Waller crystallographic thermal B-factors of the KcsA channel structure solved at 2.0 Å resolution in complex with a FAB antibody fragment<sup>1</sup> (PDB databank ID 1K4C) are compared with the results from the current molecular dynamics simulation. The B-factors of the backbone atoms of the selectivity filter KcsA are in the range of 15 to 20 Å<sup>2</sup>. In principle, the B-factors are directly related to the RMS atomic fluctuations with  $B = (8\pi^2/3) \langle \Delta R^2 \rangle$ .<sup>2,3</sup> However, interpretation of the B-factors requires some care<sup>4</sup> because the crystals were fast-frozen in liquid nitrogen<sup>1</sup> and the diffraction data was obtained under a flow of liquid nitrogen vapor according to a standard protocol (temperature around 120 to 140 K). A lower bound to the RMS fluctuations is obtained directly from the experimental B-factors, based on the assumption that all thermal motions were quenched infinitely rapidly upon fast-freezing in liquid nitrogen. This lower bound yields RMS atomic fluctuations in the range of 0.8 to 0.9 Å (data identified as 140 K in the figure). However, fast-freezing is not instantaneous on molecular timescales.<sup>4,5</sup> The RMS fluctuations at room temperature (298 K) can be estimated based on the assumption that the small sub-angstrom librations of the backbone occurring on the picosecond timescale have sufficient time to anneal to the lower temperature upon freezing (140 K). Because the thermal quadratic fluctuations  $\langle \Delta R^2 \rangle$  are linearly proportional to the effective temperature in the harmonic approximation,<sup>3</sup> the RMS fluctuations at 298 K can be estimated by scaling the RMS fluctuations at 140 K by  $(298/140)^{1/2}$ . This yields RMS atomic fluctuations in the range of 1.1 to 1.2 Å (data identified as 298 K in the figure). The results from the current molecular dynamics trajectory, shown as open symbols in the figure, falls between the lower and upper estimates from the crystallographic B-factors. An exact correspondence between MD and the estimates extracted from the B-factors is not expected due to uncertainties in the interpretation of the low temperature B-factors. The RMS thermal fluctuations of the backbone atoms of the selectivity filter of the KcsA channel are roughly on the order of 1 Å, similar to that of most proteins and much larger than the size difference between K<sup>+</sup> and Na<sup>+</sup> (0.38 Å).

## B) *Ab Initio* Calculations

All *ab initio* computations were done using Gaussian-98 program suite.<sup>6</sup> The geometry of the complex with  $K^+$  in the  $S_2$  binding site was optimized at Hartree-Fock (HF) level using the split valence 6-31G\* basis set starting from the x-ray structure.<sup>1</sup> The backbone of residues Val76-Gly77 was modeled as a glycine-dipeptide with no sidechains for a total of 37 non-hydrogen atoms requiring 1244 primitive gaussians basis functions.

The non-additivity in carbonyl-carbonyl repulsion was estimated using two N-methyl-acetamide molecules coordinating one cation. The geometry of the complex was initially optimized using density functional theory (DFT) with Becke's three-parameter hybrid method<sup>7</sup> in conjunction with the Lee, Yang, and Parr correlation functional (B3LYP)<sup>8</sup> using the split-valence 6-31++G (2d,2p) basis set. Individual contributions to interaction energies were then evaluated from single point calculations with second-order Moller-Plesset perturbation (MP2) using the split valence 6-31++G (2d,2p) basis set. Decomposition of the *ab initio* energies (Table) indicates that non-additive effects are increasingly unfavorable (repulsive) as the radius of the cation gets smaller. Induced polarization contributes an additional +3.8 kcal/mol and +4.4 kcal/mol to the NMA-NMA repulsion in the case of  $K^+$  and  $Na^+$ , respectively. Therefore, it can be anticipated that the unfavorable free energy arising from carbonyl-carbonyl repulsion would be reinforced by non-additive electronic polarization.

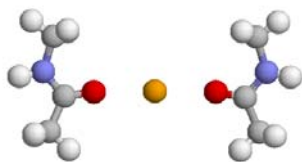


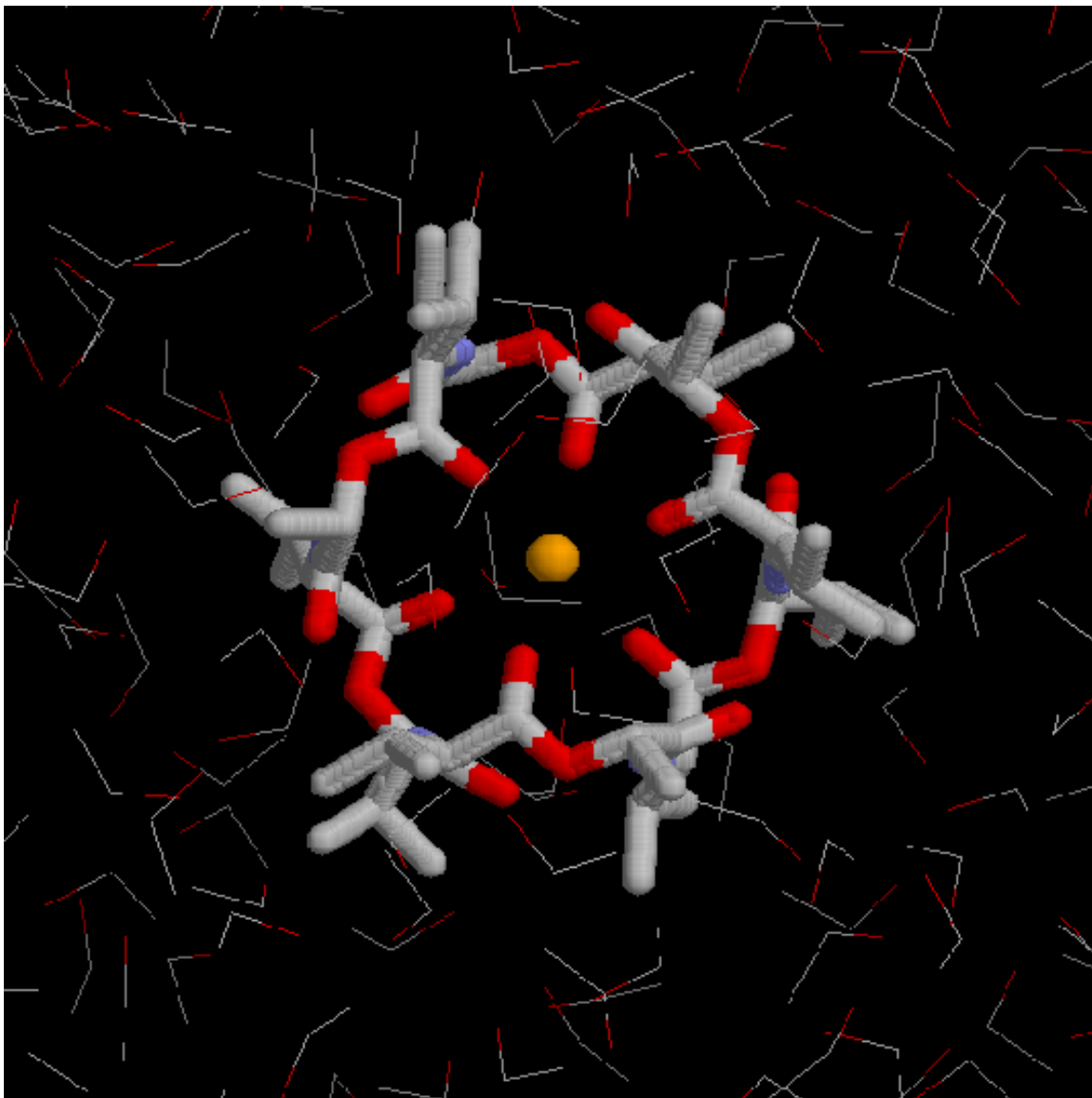
Figure. Complex of one cation with two N-methyl acetamide (NMA) molecules in the optimized geometry used to estimate the non-additive induced polarization interactions.

**Table. Energy Decomposition of non-additive interactions (kcal/mol)**

Energy term	$K^+$	$Na^+$
$\Delta E_{123}$	-56.97	-76.95
$\Delta E_1$	-25.53	-34.71
$\Delta E_2$	-31.44	-42.24
$\Delta E_3$	2.11	3.16
$\Delta E_4$	5.91	7.55
$\Delta \Delta E_{123}$	3.8	4.39
$\Delta E_{pair}$	-29.33	-39.08

Total ion-ligands interaction energy is  $\Delta E_{123} = E[\text{ion}, \text{NMA}_1, \text{NMA}_2] - E[\text{NMA}_1, \text{NMA}_2] - E[\text{ion}]$ ; Individual interaction energy between ion and 1-st NMA with accounting repulsion from the second NMA is  $\Delta E_1 = E[\text{ion}, \text{NMA}_1, \text{NMA}_2] - E[\text{NMA}_1, \text{ion}] - E[\text{ion}]$ ; interaction energy between ion and individual NMA:  $\Delta E_2 = E[\text{ion}, \text{NMA}_1] - E[\text{ion}] - E[\text{NMA}_1]$ ; Repulsion between 2 NMA in the absence of the ion is  $\Delta E_3 = E[\text{NMA}_1, \text{NMA}_2] - E[\text{NMA}_1] - E[\text{NMA}_2]$ ; Total repulsion energy between 2 NMA in presence of the ion is:  $\Delta E_4 = \Delta E_1 - \Delta E_2$ ; Non-additive correction to the electrostatic repulsion is  $\Delta \Delta E_{123} = \Delta E_4 - \Delta E_3$ ; NMA-ion pair interaction energy without non-additive correction is  $\Delta E_{pair} = \Delta E_1 - \Delta \Delta E_{123}$

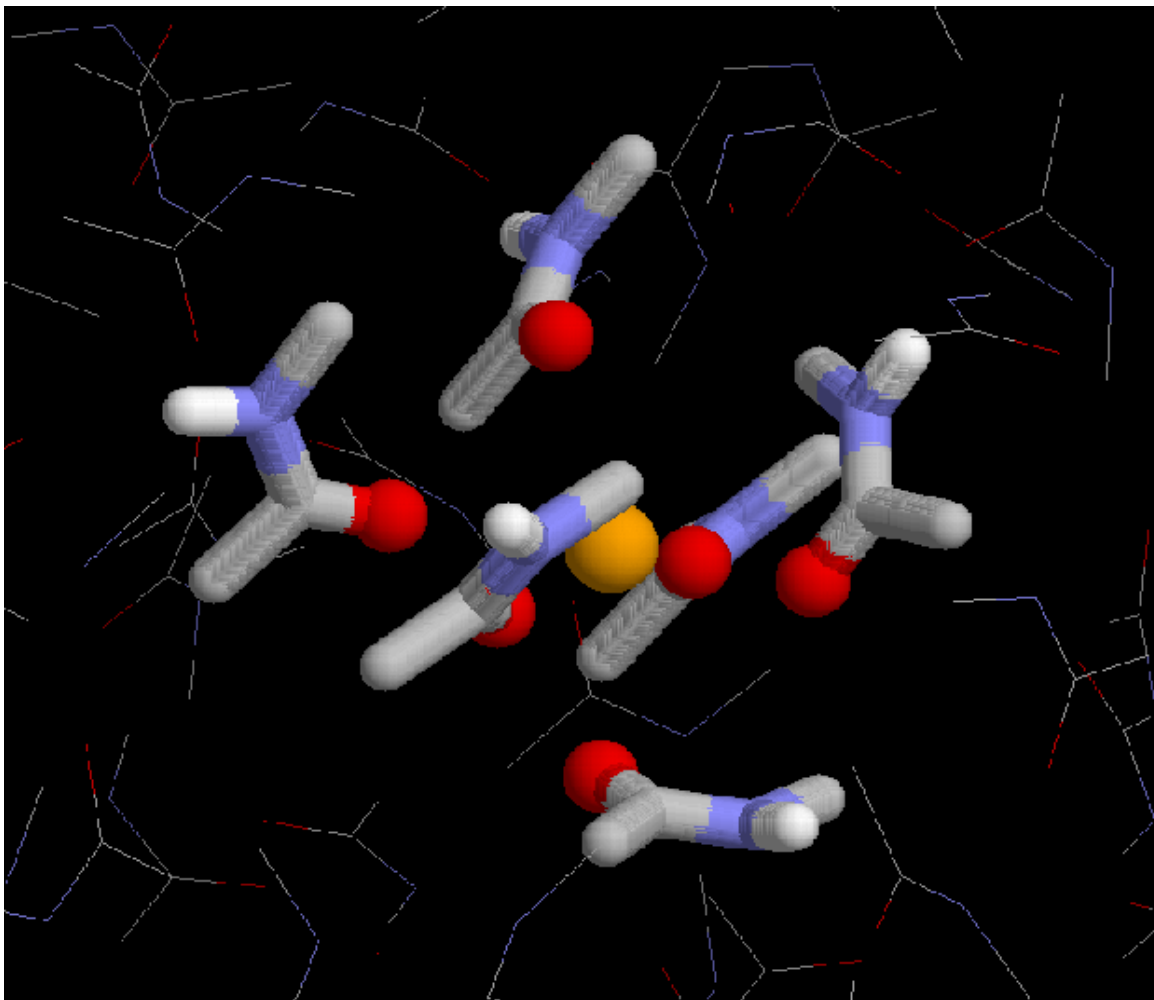
### C) Ion selectivity in valinomycin solvated in ethanol



RASMOL representation of valinomycin solvated in ethanol. The x-ray structure of a  $\text{K}^+$  valinomycin complex<sup>9,10</sup> was used to construct the initial system which was then solvated with 225 ethanol. The cation is coordinated by six carbonyl groups. The system was simulated with cubic periodic boundary conditions. The relative free energy of  $\text{K}^+$  and  $\text{Na}^+$  was calculated using molecular dynamics free energy simulations:

$$\Delta\Delta G(\text{K}^+ \rightarrow \text{Na}^+) = \left[ \left( G_{\text{valinomycin}}(\text{Na}^+) - G_{\text{bulk}}(\text{Na}^+) \right) - \left( G_{\text{valinomycin}}(\text{K}^+) - G_{\text{bulk}}(\text{K}^+) \right) \right]$$

## D) Ion solvation in liquid N-methylacetamide

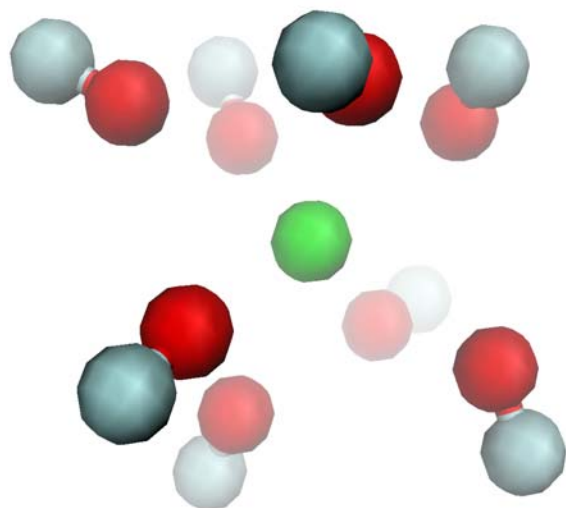


RASMOL representation of ion solvation in liquid N-methyl acetamide. Both  $K^+$  and  $Na^+$  are coordinated by six carbonyl groups in the first solvation shell in a semi-cubic geometry due to packing constraints. The system comprising one cation ( $K^+$  or  $Na^+$ ) and 150 NMA molecules was simulated with cubic periodic boundary conditions. The relative solvation free energy of  $K^+$  and  $Na^+$  was calculated using molecular dynamics free energy simulations:

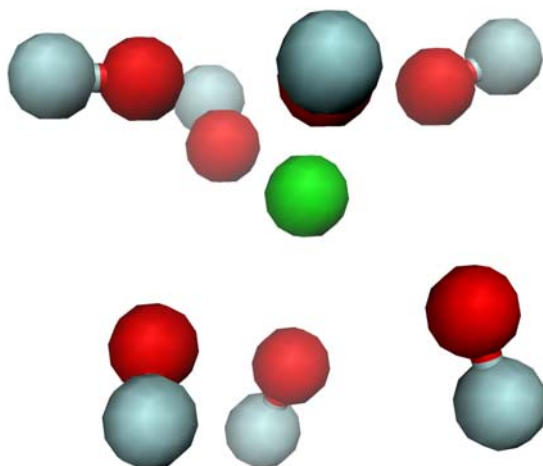
$$\Delta\Delta G(K^+ \rightarrow Na^+) = \left[ \left( G_{\text{NMA}}(Na^+) - G_{\text{water}}(Na^+) \right) - \left( G_{\text{NMA}}(K^+) - G_{\text{water}}(K^+) \right) \right]$$

### E) Ion solvation in the simplified model

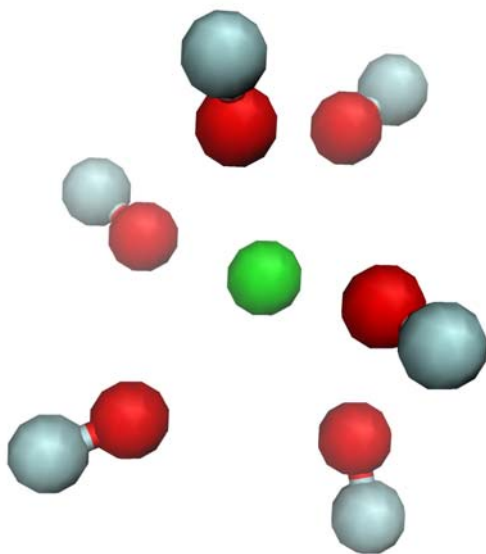
Instantaneous configurations of the freely-fluctuating carbonyls-like ligands surrounding the  $K^+$  ion at room temperature.



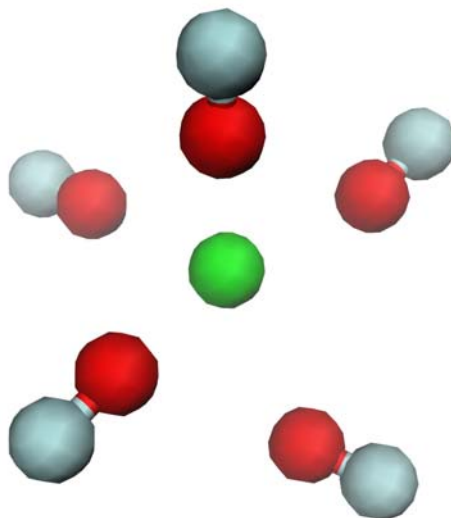
8 carbonyl-like ligands



7 carbonyl-like ligands



6 carbonyl-like ligands



5 carbonyl-like ligands

## References for supplementary material

1. Zhou, Y., Morais-Cabral, J.H., Kaufman, A. and MacKinnon, R. Chemistry of ion coordination and hydration revealed by a  $K^+$  channel-Fab complex at 2.0 Å resolution. *Nature* **414**, 43-48 (2001).
2. Halle, B. Flexibility and packing in proteins. *Proc. Natl. Acad. Sci. USA* **99**, 1274-1279 (2002).
3. Willis, B. T. M., Pryor, A.W. *Thermal vibration in crystallography* (Cambridge University Press, Cambridge, UK., 1975).
4. Halle, B. Biomolecular cryocryallography: structural changes during flash-cooling. *Proc. Natl. Acad. Sci. USA* **101**, 4793-4798 (2004).
5. Garman, E. Cool Data: quantity AND quality. *Act. Cryst. D* **55**, 1641-1653 (1999).
6. Frisch, M. J., et. al. Gaussian 98, revision A, Gaussian inc., Pittsburgh., (1998).
7. Becke, A. D. Density-functional thermochemistry. III. The role of exact exchange. *J. Chem. Phys.* **98**, 5648-5652 (1993).
8. Lee, C., Yang, W. and Parr, R.G. Development of the Colle-Salvetti correlation-energy formula into a functional of the electron density. *Phys. Rev. B* **37**, 785-789 (1988).
9. Duax, W. L., Hauptman, H., Weeks, C.M., Norton, D.A. Valinomycin crystal structure determination by direct methods. *Science* **176**, 911-914 (1972).
10. Neupert-Laves, K., Dobler, M. The crystal structure of a  $K^+$  complex of valinomycin. *Helv. Chim. Acta* **58**, 432-442 (1975).